Impact of sensor degradation on the MODIS NDVI time series

Dongdong Wang [a*], Douglas Morton [b], Jeffrey Masek [b], Aisheng Wu [c], Jyoteshwar Nagol [a], Xiaoxiong Xiong [b], Robert Levy [c], Eric Vermote [a], Robert Wolfe [b]

[a] Department of Geography, University of Maryland, College Park, MD 20742

[b] NASA Goddard Space Flight Center, Greenbelt, MD 20771

[c] Science Systems and Applications, Inc., 10210 Greenbelt Road, Lanham, MD 20706

[*]Author for Correspondence:

Dongdong Wang

Department of Geography, University of Maryland,

2181 LeFrak Hall, College Park, MD 20742, USA.

Fax: +1-301-314-9299, Phone: +1-301-405-4538, Email: ddwang@umd.edu

Submitted to Geophysical Research Letters

Abstract

Time series of satellite data provide unparalleled information on the response of vegetation to climate variability. Detecting subtle changes in vegetation over time requires consistent satellite-based measurements. Here, we evaluated the impact of sensor degradation on trend detection using Collection 5 data from the Moderate Resolution Imaging Spectroradiometer (MODIS) sensors on the Terra and Aqua platforms. For Terra MODIS, the impact of blue band (Band 3, 470nm) degradation on simulated surface reflectance was most pronounced at near-nadir view angles, leading to a 0.001-0.004 yr^{-1} decline in Normalized Difference Vegetation Index (NDVI) under a range of simulated aerosol conditions and surface types. Observed trends MODIS NDVI over North America were consistent with simulated results, with nearly a threefold difference in negative NDVI trends derived from Terra (17.4%) and Aqua (6.7%) MODIS sensors during 2002-2010. Planned adjustments to Terra MODIS calibration for Collection 6 data reprocessing will largely eliminate this negative bias in NDVI trends over vegetation.

1. Introduction

Satellite data capture changes in the land surface, atmosphere, and ocean on diurnal to decadal time scales. Large and remote areas can be monitored using satellite data, and at nearly 40 years, the lengthening time series of satellite observations offers insight into climate impacts on human and natural systems. In particular, satellite-based studies of changes in vegetation phenology from seasonal, annual, and decadal-scale temperature variability have received considerable attention in recent years (e.g., [*Myneni et al.*, 1997], [*Goetz et al.*, 2005], [*Wang et*

al., 2011]). Detecting subtle changes in vegetation characteristics requires long time series of data from well-calibrated sensors [*Slayback et al.*, 2003] and careful attention to uncertainties associated with atmospheric correction [*Nagol et al.*, 2009] and sensor degradation.

Data from the Moderate Resolution Imaging Spectroradiometer (MODIS) sensors on board the NASA Terra (2000-present) and Aqua (2002-present) satellites provide a unique opportunity to assess the consistency of satellite-based measurements. Data products from both sensors are generated using consistent algorithms, and MODIS standard products support a range of science applications (e.g. [*Esaias et al.*, 1998; *Justice et al.*, 2002; *King et al.*, 2003]). Recently, several studies have reported inconsistent results from the Terra and Aqua MODIS sensors, including estimates of ocean chlorophyll-a concentrations [Djavidnia et al., 2010] and aerosols [Levy et al., 2010]. Such discrepancies may impact the interpretation of time series or even the ability to detect time-dependent trends, especially for MODIS products that utilize data from both Terra and Aqua MODIS sensors.

Here, we analyzed the impact of sensor degradation on trends in MODIS normalized difference vegetation index (NDVI) over boreal forest and tundra cover types in North America, biomes previously identified as undergoing rapid climate-driven changes in productivity [*de Jong et al.*, 2011; *Pouliot et al.*, 2009]. We calculated degradation coefficients for each MODIS spectral band, and we propagated the time-varying trends in MODIS degradation through a simplified version of the MODIS atmospheric correction process. We then compared the simulated NDVI trends to observed trends in NDVI from the Terra and Aqua MODIS sensors over boreal North America. Our study indicates that negative NDVI trends of up to -0.004 yr^{-1} can be attributed

61 solely to degradation of the visible and near-infrared (NIR) bands aboard the Terra MODIS
62 instrument. We demonstrate the need to consider sensor calibration issues when interpreting
63 decadal scale trends in land, ocean, and atmospheric constituents.

64 **2. Data and methods**

65 **2.1 MODIS Top-of-Atmosphere reflectance**

66 Sensor degradation is a common occurrence as satellite instruments age in the harsh space
67 environment. In theory, sensor calibration using onboard apparatus can correct for sensor
68 degradation, but in practice, the solar diffuser, stimulation lamps, and stability monitors
69 needed for onboard calibration also change during mission life. A useful secondary source of
70 information is to monitor reflectance trends with "pseudo-invariant" desert targets, which
71 appear to be radiometrically and spectrally stable during the satellite era [Cosnefroy et al.,
72 1996].

73 We used MODIS C5 top-of-atmosphere (TOA) reflectance data collected over the Libya 4 desert
74 site (28.44N, 23.39E) to estimate degradation of the Terra (2000-2010) and Aqua (2002-2010)
75 MODIS sensors over time. Level 1b TOA data for MODIS Bands 1 (red), 2 (NIR), and 3 (blue)
76 were extracted from 16-day repeatable orbits over the site to maintain consistent sensor
77 viewing angles. TOA reflectances were normalized using site-specific bi-directional reflectance
78 function (BRDF) coefficients determined from the first three years of Terra and Aqua
79 observations [Wu et al., 2008]. The BRDF normalized TOA data time series for each view angle

(frame), spectral band, and mirror side were fitted using a second-order polynomial to estimate degradation for days since launch (DSL):

$$Degradation = C_0 + C_1 \cdot DSL + C_2 \cdot DSL^2 \qquad (1)$$

To estimate the impact of planned changes in sensor calibration for Collection 6 (C6) MODIS reprocessing (scheduled for late 2011), we adjusted the C5 degradation coefficients using the ratio of C5:C6 TOA reflectance for the Libya 4 site (Figure S1). Prototype C6 TOA data were generated over selected targets to evaluate the impact of calibration changes on MODIS data products. C6 data for the entire MODIS time series will not be available until at least 2012. Therefore, we also estimated the potential for continued degradation in C5 Terra data by extending the fitted degradation curves to 2013 (Figure S2).

2.2 Simulation of atmospheric radiative transfer and atmospheric correction

We used the time-dependent degradation coefficients for C5 Terra MODIS data to simulate the impact of sensor degradation on trends in NDVI over boreal North America during 2000-2010. The simulation included three major steps. First, we generated 11-year time series of TOA reflectance for forest and tundra cover types under a range of aerosol conditions, adjusting TOA values for sensor degradation over time. Our simulation approach was similar to the methods used to generate the MODIS surface reflectance product (MOD09, [Vermote et al., 2002][Vermote and Kotchenova, 2008]), with several simplifying assumptions. We used the 6S vector atmospheric radiative transfer model (Version 1.1, [Kotchenova et al., 2006]). To improve computational efficiency, we built look-up tables (LUTs) of spherical albedo (ρ), path

reflectance (r_0), and transmittance (γ). These LUTs were based on 15 aerosol optical depth (AOD) values (0.01 - 2.0), three aerosol models (continental, background desert, and biomass burning), and small angular intervals (5 degree steps for solar and view zenith angles and 10 degree steps for relative azimuth angle). These three LUTs were used to relate TOA reflectance (r) and surface reflectance (r_s) [Liang, 2004]:

$$r = r_0 + \frac{r_s}{1 - r_s \rho} \gamma \quad (2)$$

Mid-summer surface reflectance inputs for different cover types were derived from Aqua MODIS NDVI data (MYD13C1, [Huete et al., 2002]). NDVI values were binned in increments of 0.1, and mean spectral reflectance values were estimated for each NDVI bin. Using equation 2, we then estimated TOA reflectance for each NDVI bin under different aerosol conditions using the LUTs described above. Finally, TOA reflectance values for each year were multiplied by the degradation coefficients estimated for C5 Terra MODIS data to simulate the TOA reflectance observed by the sensor for each view zenith angle (VZA) and spectral band.

In the second step, simulated Terra MODIS surface reflectance values were derived from the degraded TOA reflectance values. We used a simplified Dense Dark Vegetation algorithm [Kaufman et al., 1997] to retrieve AOD. Our two simplifications were 1) direct use of Band 3 surface reflectance, rather than estimating Band 3 reflectance using other MODIS bands [Kaufman et al., 1997], since C5 Terra MODIS degradation impacts were minimal for longer wavelengths, and 2) a single estimate of AOD at 550 nm from Band 3, thereby ignoring the

119 spectrum dependence of AOD, because the aerosol model was known in our simulations.

120 Given AOD, we can solve equation (2) for surface reflectance:

121 $$r_s = \frac{r - r_0}{\gamma + (r - r_0)\rho} \qquad (3)$$

122 Finally, time series of NDVI values were calculated using the estimated red and NIR surface
123 reflectance values [*Huete et al.*, 2002] for each NDVI bin, year, and set of atmospheric
124 conditions (AOD and aerosol model).

125 **2.3 Monte Carlo simulation**

126 While the radiative transfer modeling allowed us to estimate the effect of sensor degradation
127 on an individual NDVI time series, it did not address the issue of how such degradation might
128 confound the extraction of vegetation trends from a large (e.g. continental) set of data. In
129 particular, we wished to understand whether the degradation-induced errors were significant
130 compared to the stated uncertainty (random error) of the NDVI product. To explore this issue,
131 we used a set of Monte Carlo simulations to examine the sensitivity of NDVI time series trend
132 detection to artifacts from sensor degradation. Annual time series of NDVI from 2000-2010
133 were used as inputs to the Monte Carlo simulation. Each time series had an "actual" linear
134 NDVI trend of varying magnitude (-0.02 yr^{-1} to +0.02 yr^{-1}), as well as normally-distributed
135 random errors applied to the NDVI values. The standard deviation of the random error
136 distribution was set 0.015, based on MODIS validation studies over AERONET sun photometer
137 sites (http://modis-sr.ltdri.org/). The NDVI time series with random noise were fit with a linear
138 trend, using a t-test and 95% confidence interval to identify statistically significant linear trends.

Three variables were calculated for each set of Monte Carlo simulations. The bias in trend detection was estimated using the mean of all statistically significant trends, $\mu(T_{Detected})$, and the actual trend, T_0:

$$Bias = \frac{\mu(T_{Detected}) - T_0}{T_0} \quad (4)$$

The rate of missing detections was estimated as the fraction of all time series (N) in which statistically significant trends did not have the correct positive or negative signs ($n_{correct}$):

$$Missing = 1 - \frac{n_{correct}}{N} \quad (5)$$

The rate of false detections was estimated as the fraction of all statistically significant trends (n_{sig}) in which statistically significant trends had the opposite signs ($n_{incorrect}$):

$$False = \frac{n_{incorrect}}{n_{sig}} \quad (6)$$

2.4 MODIS NDVI trends for North America

For comparison with the simulated impacts of sensor degradation described above, we mapped trends in Terra and Aqua MODIS NDVI for boreal North America during 2002-2010. We analyzed high quality NDVI values from the C5 MODIS 500m vegetation indices product (MOD13A1/MYD13A1, [*Huete et al.*, 2002]). Data were selected for four 16-day composites during the growing season (starting on day of year 177, 193, 209, and 225) to minimize impacts of vegetation phenology, and time series analyses were conducted separately for each

compositing period. Only pixels with high-quality NDVI observations in at least 6 out of the 9-year record were included in the analysis. NDVI time series were fit with a linear trend, using a t-test and 95% confidence interval to identify statistically significant linear trends. For pixels with statistically significant NDVI trends in more than one compositing period, only pixels in which all statistically significant trends had the same slope direction (positive or negative) were retained for the final map. A map of forest disturbances between 1990-2000 was used to exclude areas of fire damage or timber harvest predating the MODIS record [Masek et al., 2008], and likely disturbance areas during the MODIS era were excluded using a threshold of NDVI change between sequential observations (>0.2).

3. Results

Sensor degradation varied by spectral band, view angle, and mirror side (Figure 1, S3). Overall, Aqua MODIS Bands 1-3 showed <2% change in TOA reflectance between 2002-2010, while Terra MODIS data exhibited substantial degradation, particularly at shorter wavelengths (Figure 1, S3). Terra MODIS Band 3 had the most pronounced degradation, with a decrease of nearly 7% at near-nadir view angles over the past decade (Figure 1). Band 3 is not used directly for calculating NDVI; instead, degradation of Band 3 TOA reflectance over time will impact the calculation of surface reflectance in other spectral bands [Kotchenova et al., 2008; Vermote et al., 2002] and higher-level MODIS products, including NDVI.

Degradation of the Terra MODIS blue band resulted in decreasing NDVI trends (2000-2010) for simulated tundra and forest cover types under a range of aerosol conditions (Figure 2). Changes in NDVI arose from the decreasing trend in retrieved AOD from degraded blue TOA

177 reflectance. Three aerosol models were tested, yet the choice of aerosol model had little
178 impact on retrieved AOD values in our simulations. For a moderate (AOD = 0.2) and high (AOD =
179 0.5) aerosol loading, retrieved AOD declined by approximately 0.1 between 2000 and 2010.
180 Under the low aerosol case, retrieved AOD reached the minimum simulation value (0.01) as the
181 blue reflectance decreased over time.

182 Negative trends in NDVI varied by VZA and aerosol loading (Table 1, S1). For moderate AOD,
183 NDVI over forest and tundra declined by 0.003 yr^{-1} at near-nadir VZA but ≤0.001 yr^{-1} for VZA
184 ≥30° from nadir. Simulations with high AOD had even stronger NDVI declines from sensor
185 degradation (>0.004 yr^{-1}, Table S1). In general, rates of declining NDVI were similar for tundra
186 and forest types when comparing simulations with the same AOD and VZA (Figure 2, S4). Low
187 and high scenarios bounded the likely impacts of sensor degradation on time-varying trends in
188 Terra MODIS C5 NDVI of -0.001 ~ -0.004 yr^{-1} (see Supplemental Materials and Tables S2, S3).

189 Implementing calibration changes planned for C6 MODIS reprocessing largely eliminated trends
190 in Terra MODIS C5 NDVI from sensor degradation over 2000-2010. For moderate AOD over
191 tundra, a limited number of off-nadir view angles retained small positive NDVI trends (0.001 yr^{-1})
192 in simulations using C6 calibration information (Table S4).

193 The systematic NDVI decrease from Terra MODIS sensor degradation could bias trend detection
194 using C5 data. Based on the Monte Carlo simulations, the bias in trend detection could
195 be >500% when the actual NDVI change is small (<0.002 yr^{-1}) and the degradation rate is large (-
196 0.003 yr^{-1}). In this case, nearly all detected trends originated from sensor degradation rather
197 than actual vegetation dynamics (Figure 3). When degradation of NDVI was simulated at -0.003

198 yr^{-1}, almost half of simulated NDVI trends of +0.006 yr^{-1} could not be detected or were detected
199 with the opposite sign. Even a degradation-based NDVI decline of -0.001 yr^{-1} resulted in >50%
200 missing detections of all NDVI trends between -0.002 and +0.004 yr^{-1}. Overall, the Monte Carlo
201 simulations demonstrate that the combined impact of sensor degradation and product
202 uncertainties have a large impact on correct identification of trends in MODIS NDVI.

203 The magnitude of simulated Terra NDVI decreases matched the observed distribution of
204 positive and negative trends from Terra and Aqua MODIS data over North America. Both Terra
205 and Aqua MODIS indicated regions with statistically significant negative (browning) and positive
206 (greening) NDVI trends during 2002-2010 (Figure 4). However, there was a threefold difference
207 in the area of negative NDVI trends from Terra compared to Aqua, with large contiguous
208 regions where Terra data indicated small negative NDVI trends. NDVI trends over boreal forest
209 and tundra vegetation were small, with the mode of Aqua NDVI trend of +0.008 $year^{-1}$. Monte
210 Carlo simulations (Section 3.2) suggest that these subtle changes fall within the range of time
211 series trends that may be impacted by the combination of sensor degradation and product
212 uncertainties. The combination of subtle changes in NDVI and comparable impacts from sensor
213 degradation resulted in substantial differences in the spatial patterns of NDVI trends from Terra
214 and Aqua. For the pixels with statistically significant trends in both maps, the mean difference
215 between Terra and Aqua NDVI trends was -0.002 yr^{-1} (Figure S5), similar to the simulated
216 decline in Terra MODIS NDVI from sensor degradation.

217 **4. Discussion & Conclusions**

Based on our simulations, we expect degradation of the Terra MODIS blue band to result in negative NDVI trends over tundra and boreal forest vegetation, with greater impacts at the near-nadir VZAs favored in the MODIS reflectance and NDVI products. Previous studies based on AVHRR and Landsat data have identified greening and browning trends of 0.005-0.01 NDVI yr^{-1} in the boreal and tundra regions of North America [*de Jong et al.*, 2011; *Pouliot et al.*, 2009]. Our simulations suggest that up to half of all actual NDVI trends of this magnitude could be missed by Terra MODIS when both sensor degradation and product uncertainties are considered. Initial simulations using data processed with prototype C6 algorithms indicate no significant trends associated with sensor degradation for near-nadir VZAs. Thus, it is expected that C6 will largely fix the issues described in this paper. Until C6 data are available for the Terra MODIS time series, we suggest that users rely on Aqua MODIS data for studies of inter-annual variability in NDVI.

Studies of subtle trends in vegetation cover may be particularly sensitive to artifacts from Terra MODIS sensor degradation. Many land products select near-nadir observations where sensor degradation was most pronounced, and the small negative bias in Terra MODIS NDVI from sensor degradation may be more easily confused with real browning trends over vegetation than cloud contamination or other sensor artifacts. Many other applications will be less sensitive to artifacts from sensor degradation, such as studies that use longer wavelengths or applications based on large and persistent changes in surface reflectance associated with land cover change.

238 Terra MODIS blue band degradation may also account for observed discrepancies in AOD from
239 Terra and Aqua MODIS sensors. Levy et al. [2010] noted that Terra's AOD record showed a
240 negative trend compared to ground-based AERONET sunphotometers while comparisons
241 between AERONET and Aqua AOD showed no trend. Over land, MODIS aerosol retrieval is
242 based on three bands, including Band 3 [*Remer et al.*, 2005]. Sensitivity tests suggest that ≥3%
243 degradation of Band 3 is sufficient to explain the trend in Terra MODIS versus AERONET
244 comparison. As with studies of vegetation, C5 Aqua MODIS data should be used for studies of
245 inter-annual variability in aerosols until Band 3 degradation can be addressed in C6
246 reprocessing.

247 Sensor calibration is critical for time series analyses. Long time series desired by the science
248 community necessitate consistent calibration throughout the entire mission lifetime. In the
249 case of MODIS, calibration efforts now utilize onboard equipment, monthly lunar observations,
250 and pseudo-invariant ground targets to determine time-dependent and wavelength-dependent
251 changes in the reflective solar bands. Instrument characteristics and on-orbit malfunctions also
252 complicate sensor calibration. The observed degradation on Terra MODIS is thought to be
253 associated with on-orbit changes in the bi-directional reflectance characteristics of the solar
254 diffuser from those obtained in pre-launch tests, which is used along with measurements by the
255 solar diffuser stability monitor to derive on-orbit degradation rates. Following an anomaly with
256 the Terra MODIS solar diffuser in 2003, the solar diffuser door was fixed in the “open” position
257 to keep the instrument screen permanently in place. Since that change, the rate of Terra MODIS
258 degradation has increased. These issues highlight the importance of having multiple lines of

evidence for assessing sensor calibration, including the use of both on-board mechanisms and invariant ground targets.

Terra MODIS C5 data remain an important source of information for a range of science applications. However, time series analysis of vegetation or aerosol properties based directly or indirectly on C5 Terra MODIS Band 3 data may be sensitive to impacts of sensor degradation. Errors from sensor degradation remain within the uncertainties of the retrieval algorithm and instrument characteristics [*Vermote and Kotchenova*, 2008]. However, even small trends in sensor performance may influence time series analysis. C6 data reprocessing will likely alleviate the problems identified in this study, yet MODIS data users should consider the potential for sensor degradation to impact their analysis, given that the aging MODIS sensors will remain vulnerable to similar problems in the future.

References:

Cosnefroy, H. N., M. Leroy, and X. Briottet (1996), Selection and characterization of Saharan and Arabian desert sites for the calibration of optical satellite sensors, Remote Sensing of Environment, 58(1), 101-114.

de Jong, R., S. de Bruin, A. de Wit, M. E. Schaepman, and D. L. Dent (2011), Analysis of monotonic greening and browning trends from global NDVI time-series, Remote Sensing of Environment, 115(2), 692-702.

Djavidnia, S., F. Melin, and N. Hoepffner (2010), Comparison of global ocean colour data records, Ocean Science, 6(1), 61-76.

Esaias, W. E., et al. (1998), An overview of MODIS capabilities for ocean science observations, Ieee Transactions on Geoscience and Remote Sensing, 36(4), 1250-1265.

Goetz, S. J., A. G. Bunn, G. J. Fiske, and R. A. Houghton (2005), Satellite-observed photosynthetic trends across boreal North America associated with climate and fire disturbance, Proceedings of the National Academy of Sciences of the United States of America, 102(38), 13521-13525.

284 Huete, A., K. Didan, T. Miura, E. P. Rodriguez, X. Gao, and L. G. Ferreira (2002), Overview of the
285 radiometric and biophysical performance of the MODIS vegetation indices, Remote Sensing of
286 Environment, 83(1-2), 195-213.

287 Justice, C. O., J. R. G. Townshend, E. F. Vermote, E. Masuoka, R. E. Wolfe, N. Saleous, D. P. Roy, and J. T.
288 Morisette (2002), An overview of MODIS Land data processing and product status, Remote Sensing of
289 Environment, 83(1-2), 3-15.

290 Kaufman, Y. J., D. Tanre, L. A. Remer, E. F. Vermote, A. Chu, and B. N. Holben (1997), Operational remote
291 sensing of tropospheric aerosol over land from EOS moderate resolution imaging spectroradiometer,
292 Journal of Geophysical Research-Atmospheres, 102(D14), 17051-17067.

293 King, M. D., W. P. Menzel, Y. J. Kaufman, D. Tanre, B. C. Gao, S. Platnick, S. A. Ackerman, L. A. Remer, R.
294 Pincus, and P. A. Hubanks (2003), Cloud and aerosol properties, precipitable water, and profiles of
295 temperature and water vapor from MODIS, IEEE Transactions on Geoscience and Remote Sensing, 41(2),
296 442-458.

297 Kotchenova, S. Y., E. F. Vermote, R. Matarrese, and F. J. Klemm (2006), Validation of a vector version of
298 the 6S radiative transfer code for atmospheric correction of satellite data. Part I: Path radiance, Applied
299 Optics, 45(26), 6762-6774.

300 Kotchenova, S. Y., E. F. Vermote, R. Levy, and A. Lyapustin (2008), Radiative transfer codes for
301 atmospheric correction and aerosol retrieval: intercomparison study, Applied Optics, 47(13), 2215-2226.

302 Levy, R. C., L. A. Remer, R. G. Kleidman, S. Mattoo, C. Ichoku, R. Kahn, and T. F. Eck (2010), Global
303 evaluation of the Collection 5 MODIS dark-target aerosol products over land, Atmospheric Chemistry
304 and Physics, 10(21), 10399-10420.

305 Liang, S. L. (2004), Quantitative remote sensing of land surfaces, John Wiley & Sons, Inc, Hoboken, New
306 Jersey.

307 Masek, J. G., C. Q. Huang, R. Wolfe, W. Cohen, F. Hall, J. Kutler, and P. Nelson (2008), North American
308 forest disturbance mapped from a decadal Landsat record, Remote Sensing of Environment, 112(6),
309 2914-2926.

310 Myneni, R. B., C. D. Keeling, C. J. Tucker, G. Asrar, and R. R. Nemani (1997), Increased plant growth in the
311 northern high latitudes from 1981 to 1991, Nature, 386(6626), 698-702.

312 Nagol, J. R., E. F. Vermote, and S. D. Prince (2009), Effects of atmospheric variation on AVHRR NDVI data,
313 Remote Sensing of Environment, 113(2), 392-397.

314 Pouliot, D., R. Latifovic, and I. Olthof (2009), Trends in vegetation NDVI from 1km AVHRR data over
315 Canada for the period 1985-2006, International Journal of Remote Sensing, 30(1), 149-168.

316 Remer, L. A., et al. (2005), The MODIS aerosol algorithm, products, and validation, Journal of the
317 Atmospheric Sciences, 62(4), 947-973.

Slayback, D. A., J. E. Pinzon, S. O. Los, and C. J. Tucker (2003), Northern hemisphere photosynthetic trends 1982-99, Global Change Biology, 9(1), 1-15.

Vermote, E. F., and S. Kotchenova (2008), Atmospheric correction for the monitoring of land surfaces, Journal of Geophysical Research-Atmospheres, 113(D23).

Vermote, E. F., N. Z. El Saleous, and C. O. Justice (2002), Atmospheric correction of MODIS data in the visible to middle infrared: first results, Remote Sensing of Environment, 83(1-2), 97-111.

Wang, X. H., S. L. Piao, P. Ciais, J. S. Li, P. Friedlingstein, C. Koven, and A. P. Chen (2011), Spring temperature change and its implication in the change of vegetation growth in North America from 1982 to 2006, Proceedings of the National Academy of Sciences of the United States of America, 108(4), 1240-1245.

Wu, A., A. Angal, X. Xiong, and C. Cao (2008), Monitoring MODIS calibration stability of visible and near-IR bands from observed top-of-atmosphere BRDF-normalized reflectances over Libyan Desert and Antarctic surfaces, Proc. SPIE 7081, 708113.

Tables and figures

Table 1. Annual trends in simulated Terra MODIS C5 NDVI during 2000-2010 over tundra (NDVI = 0.65) based on moderate aerosol loading (AOD = 0.2). Results were calculated separately for each view zenith angle (VZA) and mirror side (MS) using three different aerosol models. Negative VZAs refer to pixels from the beginning of a scan line to nadir; positive VZAs indicate pixels from nadir to the end of a scan line.

View Zenith Angle		-51	-42	-32	-28	-18	-11	-3	9	17	31	43	52
MS1	Continental	*	-0.0008	-0.0008	-0.0012	-0.0023	-0.0031	-0.0027	-0.0023	-0.0011	-0.0010	0.0023	0.0034
	Desert	*	-0.0008	-0.0008	-0.0012	-0.0023	-0.0031	-0.0027	-0.0023	-0.0011	-0.0010	0.0023	0.0034
	Bio Burning	*	-0.0006	-0.0007	-0.0010	-0.0019	-0.0028	-0.0024	-0.0021	-0.0009	-0.0008	0.0022	0.0032
MS2	Continental	0.0003	*	-0.0007	-0.0019	-0.0023	-0.0033	-0.0030	-0.0022	-0.0016	-0.0013	0.0031	0.0053
	Desert	0.0003	*	-0.0007	-0.0018	-0.0023	-0.0033	-0.0031	-0.0022	-0.0016	-0.0013	0.0031	0.0053
	Bio Burning	0.0003	*	-0.0005	-0.0016	-0.0020	-0.0029	-0.0027	-0.0019	-0.0014	-0.0011	0.0028	0.0048

* no significant trend detected

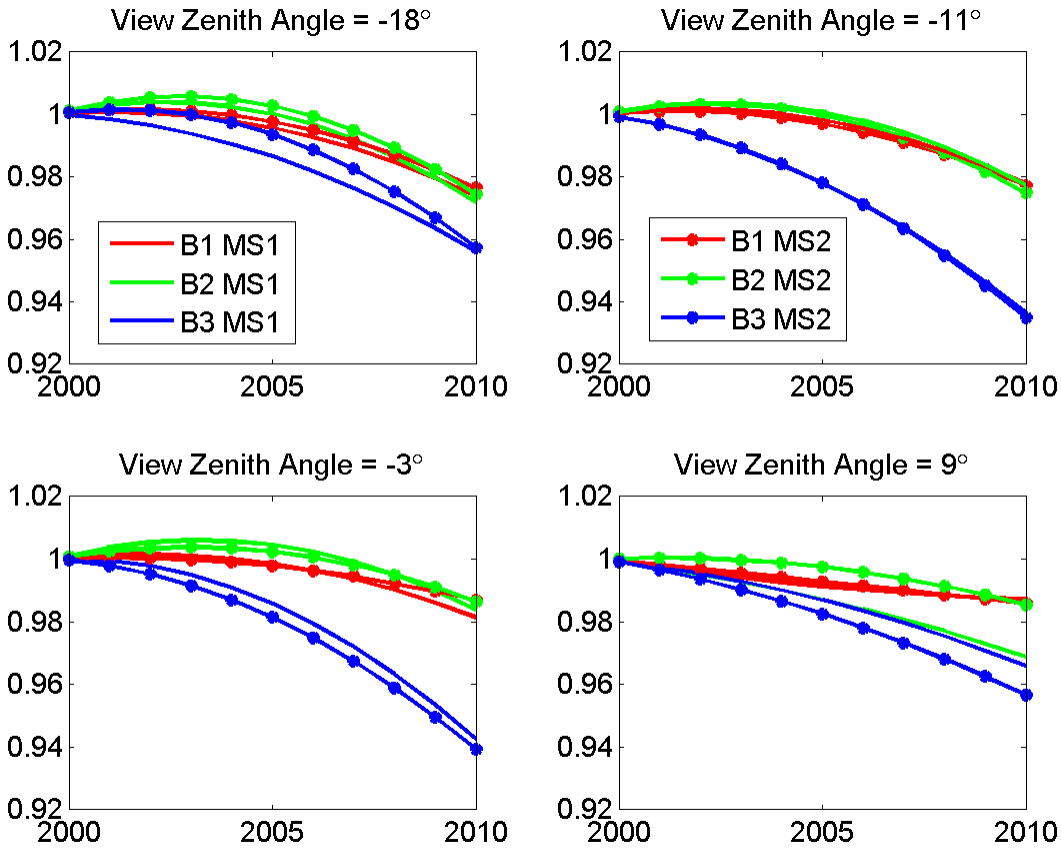

340

341 Figure 1. Fitted degradation coefficients for Terra MODIS C5 red (B1), NIR (B2), and blue (B3) top-of-
342 atmosphere reflectance using equation 1. Degradation coefficients were calculated separately for data
343 from Mirror Side 1 (MS1) and Mirror Side 2 (MS2). Additional VZAs are shown in Figure S1.

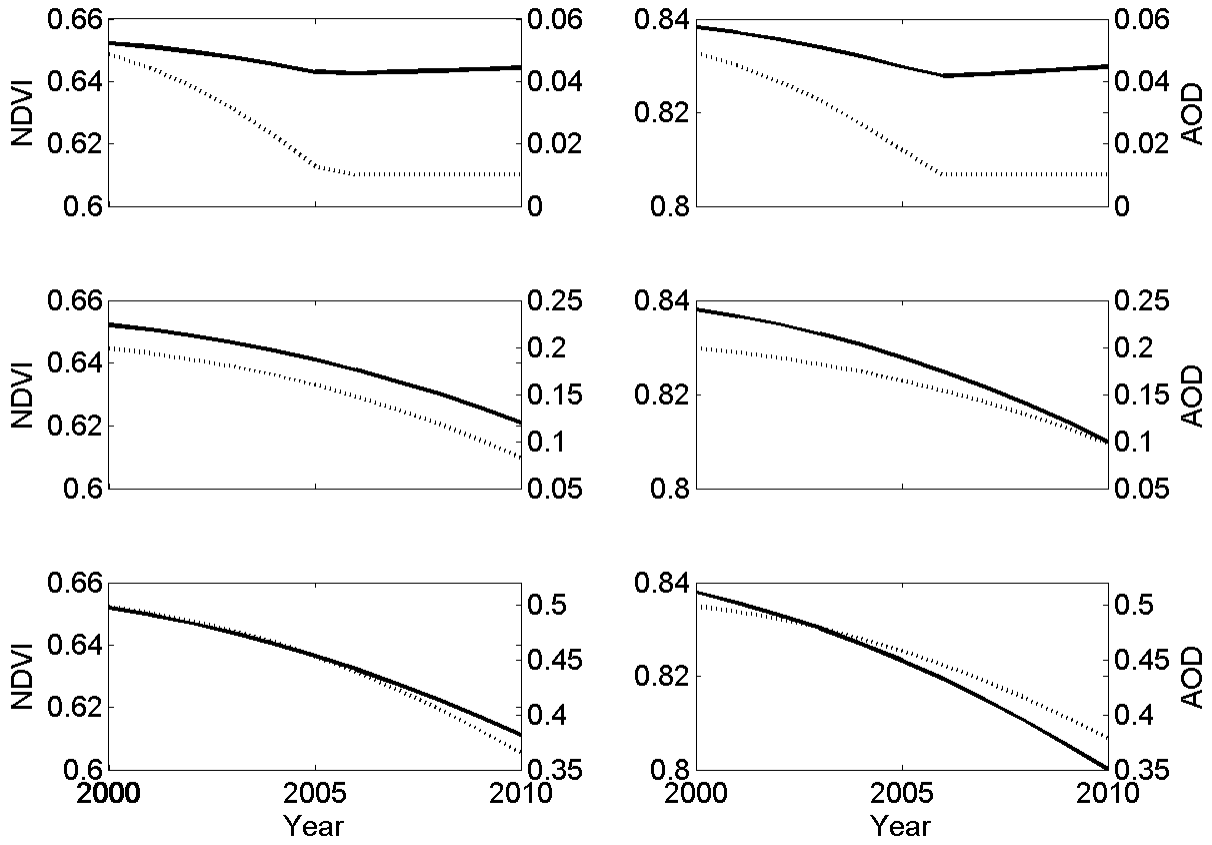

344

345 Figure 2. Simulated Terra MODIS C5 NDVI (solid lines) and AOD (dashed lines) time series for near-nadir
346 observations (VZA=-11) of tundra (left) and forest (right) during 2000-2010 with low (0.05, top),
347 moderate (0.2, middle), and high (0.5, bottom) AOD. Simulated NDVI and AOD time series for all VZAs
348 are shown in Figure S4.

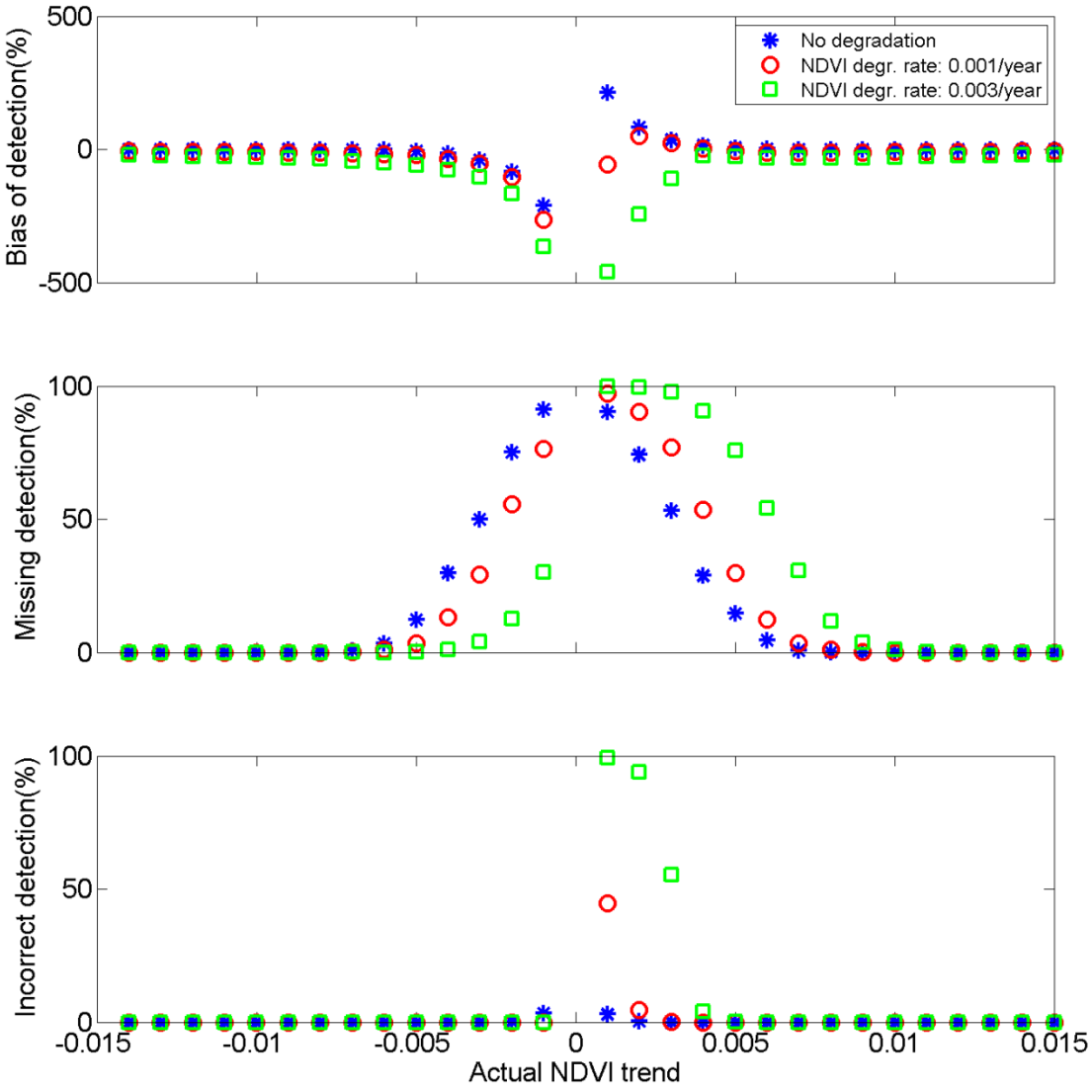

Figure 3. Monte Carlo simulation results for the combined impacts of NDVI degradation and NDVI uncertainty (0.015) on trend detection. Detection bias (top), percentage of missing detections (middle), and percentage of false detections (bottom) were summarized for all statistically significant linear trends for different actual NDVI trend levels.

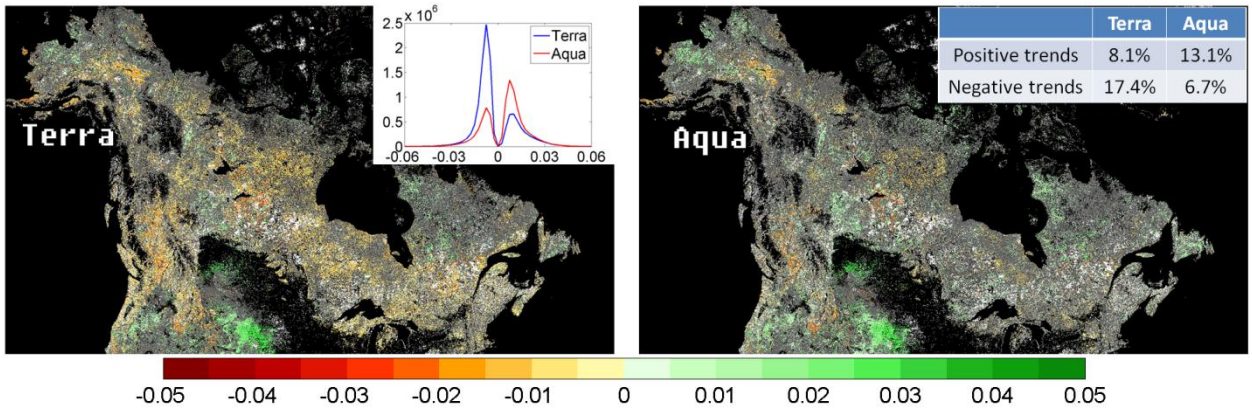

354

355 Figure 4. Trends in Terra and Aqua MODIS NDVI over North America 2002-2010. Recent disturbances
356 from fire and wood harvest appear white, while water, cropland, and barren land cover types appear
357 black. Inset panels summarize statistically significant NDVI trends over land from each time series.